



ERV1/ChemR23 Signaling Protects Against Atherosclerosis by Modifying Oxidized Low-Density Lipoprotein Uptake and Phagocytosis in Macrophages

BACKGROUND: In addition to enhanced proinflammatory signaling, impaired resolution of vascular inflammation plays a key role in atherosclerosis. Proresolving lipid mediators formed through the 12/15 lipoxygenase pathways exert protective effects against murine atherosclerosis. n-3 Polyunsaturated fatty acids, including eicosapentaenoic acid (EPA), serve as the substrate for the formation of lipid mediators, which transduce potent anti-inflammatory and proresolving actions through their cognate G-protein-coupled receptors. The aim of this study was to identify signaling pathways associated with EPA supplementation and lipid mediator formation that mediate atherosclerotic disease progression.

METHODS: Lipidomic plasma analysis were performed after EPA supplementation in *ApoE*^{-/-} mice. *Erv1/Chemr23*^{-/-}*x**ApoE*^{-/-} mice were generated for the evaluation of atherosclerosis, phagocytosis, and oxidized low-density lipoprotein uptake. Histological and mRNA analyses were done on human atherosclerotic lesions.

RESULTS: Here, we show that EPA supplementation significantly attenuated atherosclerotic lesion growth induced by Western diet in *ApoE*^{-/-} mice and was associated with local cardiovascular n-3 enrichment and altered lipoprotein metabolism. Our systematic plasma lipidomic analysis identified the resolvin E1 precursor 18-monohydroxy EPA as a central molecule formed during EPA supplementation. Targeted deletion of the resolvin E1 receptor *Erv1/Chemr23* in 2 independent hyperlipidemic murine models was associated with proatherogenic signaling in macrophages, increased oxidized low-density lipoprotein uptake, reduced phagocytosis, and increased atherosclerotic plaque size and necrotic core formation. We also demonstrate that in macrophages the resolvin E1-mediated effects in oxidized low-density lipoprotein uptake and phagocytosis were dependent on *Erv1/Chemr23*. When analyzing human atherosclerotic specimens, we identified ERV1/ChemR23 expression in a population of macrophages located in the proximity of the necrotic core and demonstrated augmented ERV1/ChemR23 mRNA levels in plaques derived from statin users.

CONCLUSIONS: This study identifies 18-monohydroxy EPA as a major plasma marker after EPA supplementation and demonstrates that the ERV1/ChemR23 receptor for its downstream mediator resolvin E1 transduces protective effects in atherosclerosis. ERV1/ChemR23 signaling may represent a previously unrecognized therapeutic pathway to reduce atherosclerotic cardiovascular disease.

Andres Laguna-Fernandez, PhD
Antonio Checa, PhD
Miguel Carracedo, MSc
Gonzalo Artiach, MSc
Marcelo H. Petri, MD, PhD
Roland Baumgartner, PhD
Maria J. Forteza, PhD
Xintong Jiang, MD, PhD
Teodora Andonova, MSc
Mary E. Walker, MSc
Jesmond Dalli, PhD
Hildur Arnardottir, PhD
Anton Gisterå, MD, PhD
Silke Thul, PhD
Craig E. Wheelock, PhD
Gabrielle Paulsson-Berne, PhD
Daniel F.J. Ketelhuth, PhD
Göran K. Hansson, MD, PhD
Magnus Bäck, MD, PhD

Key Words: atherosclerosis
■ lipoproteins, LDL ■ macrophages
■ phagocytosis

Sources of Funding, see page 1704

© 2018 The Authors. *Circulation* is published on behalf of the American Heart Association, Inc., by Wolters Kluwer Health, Inc. This is an open access article under the terms of the [Creative Commons Attribution Non-Commercial-NoDeriv](#) License, which permits use, distribution, and reproduction in any medium, provided that the original work is properly cited, the use is noncommercial, and no modifications or adaptations are made.

<https://www.ahajournals.org/journal/circ>

Clinical Perspective

What Is New?

- This study identifies 18-monohydroxy eicosapentaenoic acid as a major plasma lipid metabolite formed during omega-3 supplementation with eicosapentaenoic acid to hyperlipidemic mice.
- 18-Monohydroxy eicosapentaenoic acid is the precursor for the proresolving lipid mediator resolvin E1, which in the present study was shown to regulate critical atherosclerosis-related functions in macrophages through its downstream signaling receptor, ERV1/ChemR23, to transduce protective effects in atherosclerosis.

What Are the Clinical Implications?

- The controversy around the cardioprotective effects of omega-3 polyunsaturated fatty acids urges studies of the mechanisms involved.
- Optimizing treatments for stimulating the resolvin E1 and ERV1/ChemR23 signaling axis may be a potential therapeutic pathway to reduce atherosclerotic cardiovascular disease.

Atherosclerotic lesion development in response to elevated levels of cholesterol-rich lipoproteins is characterized by proinflammatory signaling.¹ Indeed, it was recently demonstrated that blocking proinflammatory signaling without altering lipid levels reduces the risk of recurrent cardiovascular events.² Impaired resolution of vascular inflammation plays a key role in atherosclerosis,^{3,4} and proresolving lipid mediators formed through the 12/15 lipoxygenase pathways exert protective effects against murine atherosclerosis.³⁻⁵

n-3 Polyunsaturated fatty acids (PUFAs), principally eicosapentaenoic acid (EPA) and docosahexaenoic acid, serve as the substrate for the formation of anti-inflammatory and proresolving lipid mediators with potential beneficial effects in multiple inflammatory diseases, including atherosclerosis.^{3,4} EPA metabolism leads to the formation of 18-monohydroxy EPA (18-HEPE),⁶ the precursor for the lipid mediator resolvin E1 (RvE1), which transduces its proresolving actions by means of the G-protein-coupled receptor referred to as ERV1/ChemR23.⁷ Indeed, overexpression of ERV1/ChemR23 enhances the effects of RvE1 in different animal models.^{8,9}

In addition, in vivo administration of RvE1 and 15-epi lipoxin A4 to hyperlipidemic mice reduces atherosclerosis progression.^{10,11} Nonetheless, whether and how these lipid mediators and their specific receptors participate in the observed effects of n-3 PUFA supplementation in cardiovascular disease remain largely unexplored.

Deepening the comprehension of the metabolism and signaling associated with n-3 PUFA supplementation is important to understand how to appropriately

stimulate specific pathways for therapeutic purposes. In addition, such understanding may also provide explanations for the inconsistent results obtained in clinical trials evaluating the role of n-3 PUFA supplementation in cardiovascular prevention.¹²

The aim of this study was to identify signaling pathways associated with EPA supplementation and lipid mediator formation that mediate atherosclerotic disease progression. When addressing this question, we identified the RvE1 precursor 18-HEPE as a major plasma marker after EPA supplementation, associated with increased tissue concentrations of its bioactive metabolite RvE1. Therefore, we subsequently generated 2 independent *Erv1/Chemr23*-deficient hyperlipidemic murine strains, which exhibited accelerated atherosclerosis. In addition, we demonstrated that in macrophages the RvE1-mediated effects in oxidized (ox) low-density lipoprotein (LDL) uptake and phagocytosis are dependent on *Erv1/Chemr23*. Finally, we provide the translational implications by determining ERV1/ChemR23 expression patterns in human atherosclerosis and their association with statin use.

METHODS

Animal Studies

Animal experiments were conducted in accordance with guidelines from the Directive 2010/63/EU of the European Parliament and were approved by the Ethical Committee of Northern Stockholm. Details about diets (Table I in the online-only Data Supplement), experimental animals (Table II and Figure 1 in the online-only Data Supplement), materials (Table III in the online-only Data Supplement), and supplemental methods are provided online. The data, analytical methods, and study materials will be made available to other researchers for the purposes of reproducing the results or replicating the procedure (available at the authors' laboratories).

Human Studies

Informed consent was obtained from all subjects. The investigation was approved by the Ethical Committee of Northern Stockholm and was in agreement with the Declaration of Helsinki.

Statistical Analysis

Experimental results are presented as mean±SEM and clinical parameters as median (interquartile range). All statistical analyses were 2 sided. Adjusted *P* values are shown for multiple comparisons.

RESULTS

EPA Administration Modifies Fatty Acid Composition in Tissues From *ApoE*^{-/-} Mice

ApoE^{-/-} mice fed a Western diet supplemented with EPA for 4 weeks exhibited a significant increase in

n-3 PUFAs and a significant reduction in n-6 PUFAs in myocardium, spleen, and skeletal muscle compared with animals fed a Western diet. In those tissues, EPA content was significantly increased by 388-, 384-, and 706-fold, respectively (Table 1).

EPA Supplementation Attenuates Diet-Induced Atherosclerosis in *Apoe*^{-/-} Mice

EPA supplementation significantly attenuated atherosclerotic lesion growth induced by Western diet in both the aortic arch (Figure 1A and 1B) and the aortic root (Figure 1C).

No significant differences in blood counts resulting from the different diets were observed. Compared with the animals fed a chow diet, higher body weight was observed in the animals fed a Western diet independently of EPA supplementation (Table II in the online-only Data Supplement).

Nonfasting plasma analyses revealed that the EPA-supplemented animals exhibited a trend toward higher triglyceride levels than the animals fed a Western diet or a chow diet. No significant difference was found between the animals fed a Western and those fed a chow diet. Total plasma cholesterol levels were significantly higher in the animals fed a Western diet than in those fed a chow diet. Despite a trend, total plasma cholesterol levels in the EPA-supplemented animals were not significantly different from those

in animals fed a Western or a chow diet (Table 2). Further investigation of the different lipoprotein fractions revealed that compared with Western diet, EPA supplementation significantly decreased very-low-density lipoprotein (VLDL) cholesterol to levels similar to those exhibited by the animals fed a chow diet. LDL and high-density lipoprotein fractions remained similar among the different groups (Figure IIA in the online-only Data Supplement). In addition, EPA supplementation caused a significant decrease of the hepatic mRNA levels of 3-hydroxy-3-methyl-glutaryl-coenzyme A reductase (*Hmgcr*; Figure IIB in the online-only Data Supplement).

EPA Supplementation Reshapes the Lipid Mediator Profile in Plasma of *Apoe*^{-/-} Mice: Identification of Components of the *Erv1/Chemr23* Signaling Pathway

The experimental diet groups were separated in a principal component analysis model according to their lipid mediator profile (Figure 1D). A heat map analysis showed that EPA supplementation significantly increased the levels of most n-3-derived lipid mediators and reduced those of n-6-derived lipid mediators compared with the animals fed a chow or a Western diet (Figure IC in the online-only Data Supplement). Variable importance for projection scores were calculated from the partial least-squares discriminant analysis (Figure IID

Table 1. EPA Supplementation Modifies Fatty Acid Composition in Different Tissues of *Apoe*^{-/-} Mice

| | Myocardium | | | Spleen | | | Skeletal Muscle | | |
|-----------------------------------|-------------|--------------|--------------|-------------|--------------|--------------|-----------------|--------------|--------------|
| | WD (n=3) | WD+EPA (n=3) | WD+EPA vs WD | WD (n=3) | WD+EPA (n=3) | WD+EPA vs WD | WD (n=3) | WD+EPA (n=3) | WD+EPA vs WD |
| Fatty acid, % of total | Mean±SEM | Mean±SEM | P Value | Mean±SEM | Mean±SEM | P Value | Mean±SEM | Mean±SEM | P Value |
| Palmitic acid, C16_0 | 14.42±0.17 | 14.64±0.27 | 0.5403 | 26.55±0.33 | 27.38±0.42 | 0.1985 | 23.79±0.68 | 25.09±0.69 | 0.252 |
| Stearic acid, C18_0 | 16.36±0.43 | 18.32±0.53 | 0.0463* | 14.4±0.24 | 11.3±0.92 | 0.0312* | 7.25±0.46 | 6.72±0.17 | 0.3533 |
| Oleic acid, C18_1n9 | 15.55±1.3 | 9.217±0.52 | 0.0108* | 19.17±0.89 | 23.33±3.45 | 0.3086 | 41.59±3.93 | 35.56±0.68 | 0.2055 |
| Linoleic acid, C18_2n6 | 16.03±0.62 | 10.64±0.85 | 0.0068* | 6.24±0.17 | 6.73±0.35 | 0.2933 | 8.6±0.9 | 8.13±1.40 | 0.7907 |
| α-Linolenic acid, C18_3n3 | 0.07±0.01 | 0.09±0.01 | 0.1447 | 0.06±0.01 | 0.13±0.02 | 0.0168* | 0.13±0.01 | 0.19±0.02 | 0.0836 |
| Eicosatrienoic acid, C20_3n6 | 0.78±0.03 | 0.24±0.01 | 0.0001* | 0.92±0.04 | 0.21±0.01 | 0.0001* | 0.59±0.05 | 0.17±0.01 | 0.0011* |
| Arachidonic acid, C20_4n6 | 12.14±0.28 | 6.88±0.4 | 0.0004* | 20.4±0.38 | 5.35±0.43 | <0.0001* | 7.92±0.79 | 4.18±0.11 | 0.0098* |
| EPA, C20_5n3 | 0.013±0.003 | 5.04±0.45 | 0.0004* | 0.036±0.003 | 13.83±0.93 | 0.0001* | 0.01±0.001 | 7.06±0.4 | <0.0001* |
| Docosatetraenoic acid, C22_4n6 | 0.54±0.02 | 0.06±0.003 | <0.0001* | 3.4±0.07 | 0.17±0.01 | <0.0001* | 0.46±0.03 | 0.1±0.02 | 0.0003* |
| Docosapentaenoic acid n6, C22_5n6 | 2.59±0.17 | 0.28±0.02 | 0.0002* | 0.75±0.03 | 0.043±0.003 | <0.0001* | 1.09±0.17 | 0.3±0.01 | 0.0154* |
| Docosapentaenoic acid n3, C22_5n3 | 0.42±0.02 | 8.51±0.65 | 0.0003* | 0.54±0.01 | 7.76±1.07 | 0.0025* | 0.22±0.02 | 4.7±0.24 | <0.0001* |
| Docosahexaenoic acid, C22_6n3 | 19±0.96 | 24.7±0.1 | 0.0041* | 3.72±0.17 | 1.57±0.07 | 0.0004* | 6.26±0.74 | 6.27±0.96 | 0.9938 |

EPA indicates eicosapentaenoic acid; and WD, Western diet.

Gas chromatography analyses of tissue homogenates shows fatty acid content in myocardium, spleen, and skeletal muscle from *Apoe*^{-/-} mice fed a Western diet 0.15% cholesterol or a Western diet 0.15% cholesterol supplemented with 5% EPA for 4 weeks (n=3).

*Significant ($P<0.05$).

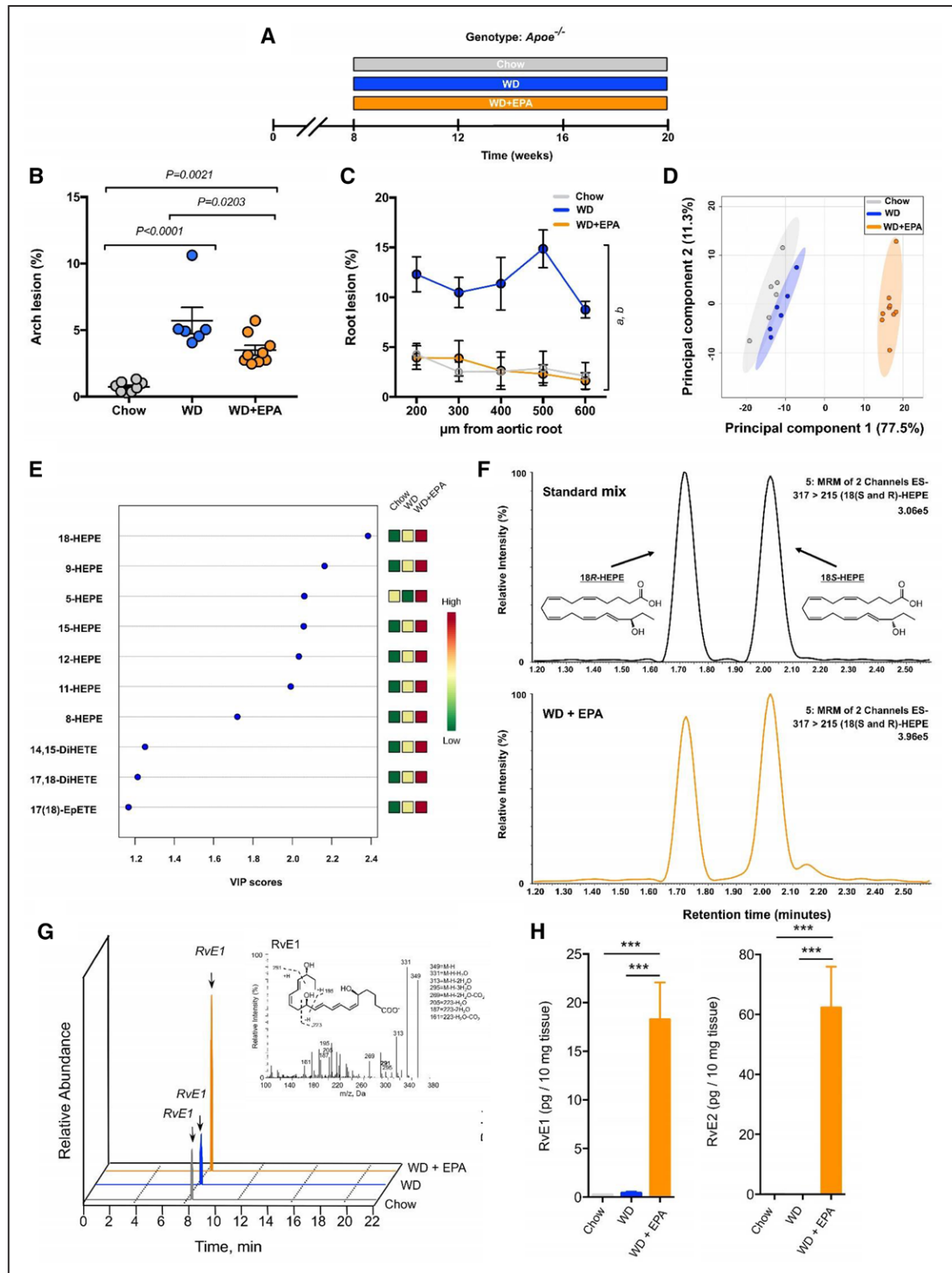


Figure 1. Eicosapentaenoic acid (EPA) supplementation inhibits diet-induced atherosclerosis and reshapes the lipid mediator profile in plasma of *ApoE*^{-/-} mice.

A, *ApoE*^{-/-} mice were fed a chow diet (light gray), a Western diet (WD; 0.15% cholesterol; dark gray), or a WD supplemented with 5% EPA (WD+EPA; medium gray) for 12 weeks. **B**, Atherosclerotic lesion size determined as percent of Sudan IV staining of the aortic arch (data presented as mean±SEM; 1-way ANOVA followed by Tukey multiple-comparison test; n=8 versus 6 versus 9) and **(C)** as percent of Oil Red O staining at different levels of the aortic root (data presented as mean±SEM; 2-way ANOVA followed by Tukey multiple-comparison test; n=8 versus 6 versus 9; ^aWD vs chow, *P*<0.0001; ^bWD vs WD+EPA, *P*<0.0001). **D**, Two-dimensional principal component analysis of lipid mediators in plasma. Colored spherical areas display 95% confidence region of respective experimental diets. **E**, Variable importance in projection (VIP) scores of 10 most significant lipid mediators explaining differences in plasma lipid mediator profile between diets. **F**, Typical example of a chromatogram for chiral assessment of 18-monohydroxy EPA (18-HEPE) in plasma of WD+EPA samples and its comparison with a standard containing equal amounts of 18*R*-HEPE and 18*S*-HEPE enantiomers. **G**, Multiple-reaction monitoring chromatograms depicting the relative quantities of resolvin (Rv) E1 in spleens from mice fed chow, WD, and WD+EPA. Inset shows tandem mass spectrometry spectrum used in the identification of RvE1. **H**, Splenic concentrations of RvE1 and RvE2 (n= 4 mice per group).

Table 2. Nonfasting Plasma Triglycerides and Total Cholesterol Concentrations

| | Concentration, mmol/L | | | P Value |
|-------------------|-----------------------|-------------|--------------|---------|
| | Chow (n=8) | WD (n=6) | WD+EPA (n=9) | |
| Triglycerides | 1.66±0.05 | 1.28±0.09 | 4.60±1.49 | 0.07 |
| Total cholesterol | 7.34±1.14 | 16.70±2.63* | 9.21±2.89 | 0.03† |

Values are mean±SEM. EPA indicates eicosapentaenoic acid; and WD, Western diet.

* $P<0.05$ versus chow.

†Significant ($P<0.05$).

in the online-only Data Supplement) and identified 18-HEPE as a critical molecule explaining the differences in plasma lipid mediator profile caused by dietary EPA supplementation (Figure 1E).

Chiral liquid chromatography/tandem mass spectrometry-based lipidomics revealed that the enantiomeric excess was $6.01\pm 1.17\%$ with 53% 18S-HEPE and 47% 18R-HEPE in the plasma of animals receiving EPA supplementation (Figure 1F). These enantiomers serve as the precursors of 18S-RvE1 and 18R-RvE1, 2 short-lived and locally produced lipid mediators with biological actions that are transduced mainly by the receptor ERV1/ChemR23. General lipid profiling methods¹³ were unable to detect RvE1 in either plasma or tissue (data not shown). However, analysis of the two 18-HEPE metabolites RvE1 and RvE2 by a targeted lipidomics approach¹⁴ revealed significant increases in RvE1 and RvE2 in spleens derived from EPA-supplemented compared with Western diet-fed mice (Figure 1G and 1H).

ErV1/Chemr23 mRNA expression was identified in the aorta of the animals, being significantly higher in the chow group than in the others (Figure IIE in the online-only Data Supplement).

Chemerin, another precursor for ERV1/ChemR23 ligands, was detected in the plasma of the 3 groups, with significantly higher levels in the Western diet group than in the chow diet group, and was not significantly altered by EPA supplementation (Figure IIF in the online-only Data Supplement).

Targeted Deletion of *ErV1/Chemr23* Enhances Atherosclerosis in *Apoe*^{-/-} Mice

After 8 weeks on a Western diet, *Apoe*^{-/-}*ErV1/Chemr23*^{-/-} mice exhibited larger atherosclerotic lesions in the aortic arch (Figure 2A and 2B) and the aortic root (Figure 2C) than the control group. No differences in blood counts, weight (Table II in the online-only Data Supplement), plasma triglycerides (1.25 ± 0.24 versus 1.22 ± 0.22 mmol/L; $P=0.79$), total cholesterol (10.63 ± 1.87 versus 11.61 ± 1.38 mmol/L; $P=0.31$), and

lipoprotein profile (Figure 2D) were found between the 2 genotypes.

After 12 weeks, *Apoe*^{-/-}*ErV1/Chemr23*^{-/-} mice exhibited larger atherosclerotic lesions in the aortic arch than the control group (Figure 2E) and similar levels in the aortic root (Figure 2F). No differences in blood counts, weight (Table II in the online-only Data Supplement), plasma triglycerides (1.29 ± 0.2 versus 1.75 ± 0.55 mmol/L; $P=0.16$), total cholesterol levels (16.70 ± 5.27 versus 22.27 ± 3.4 mmol/L; $P=0.13$), or lipoprotein profile (Figure 2G) were found between the 2 genotypes. A second group of animals under the same conditions verified these findings (data not shown).

Targeted Deletion of *ErV1/Chemr23* Changes Atherosclerotic Plaque Composition and the Expression of Genes Involved in Lesion Development

The proportion of lesion area containing CD68⁺ macrophages was significantly increased in *Apoe*^{-/-}*ErV1/Chemr23*^{-/-} mice compared with the control group (Figure 2H). Similar numbers of CD4⁺ (Figure 2I) and CD8⁺ (Figure 2J) T cells were identified in the lesions of the 2 genotypes.

Comparative quantitative polymerase chain reaction analyses in abdominal aortas of the 2 genotypes revealed differential expression of genes involved in critical functions associated with atherosclerosis. More specifically, *Apoe*^{-/-}*ErV1/Chemr23*^{-/-} mice exhibited significantly increased mRNA levels of genes involved in lipid metabolism and lipoprotein uptake: LDL receptor (*Ldlr*), VLDL receptor (*Vldlr*), and sortilin 1 (*Sort1*); significantly reduced mRNA levels for receptors involved in phagocytosis: macrophage receptor with collagenous structure (*Marco*) and T-cell immunoglobulin and mucin domain containing 4 (*Timd4*); and significantly increased mRNA levels of proinflammatory genes: osteoprotegerin (*Opg*) and Toll-like receptor 4 (*Tlr4*), accompanied by a reduction in mRNA levels of the anti-inflammatory gene interleukin 10 (*Il-10*; Figure 2K).

Apoe^{-/-}*ErV1/Chemr23*^{-/-} Macrophages Exhibit Increased oxLDL Uptake and Decreased Phagocytosis.

Apoe^{-/-}*ErV1/Chemr23*^{-/-} peritoneal macrophages exhibited increased intracellular lipid content after 24 hours of incubation with oxLDL compared with those derived from control mice (Figure 3A). Experiments using fluorescent oxLDL showed that macrophages lacking *ErV1/Chemr23* exhibited a significant continued increase in oxLDL uptake for up to 60 hours (Figure 3B and Movie I in the online-only Data Supplement). RvE1

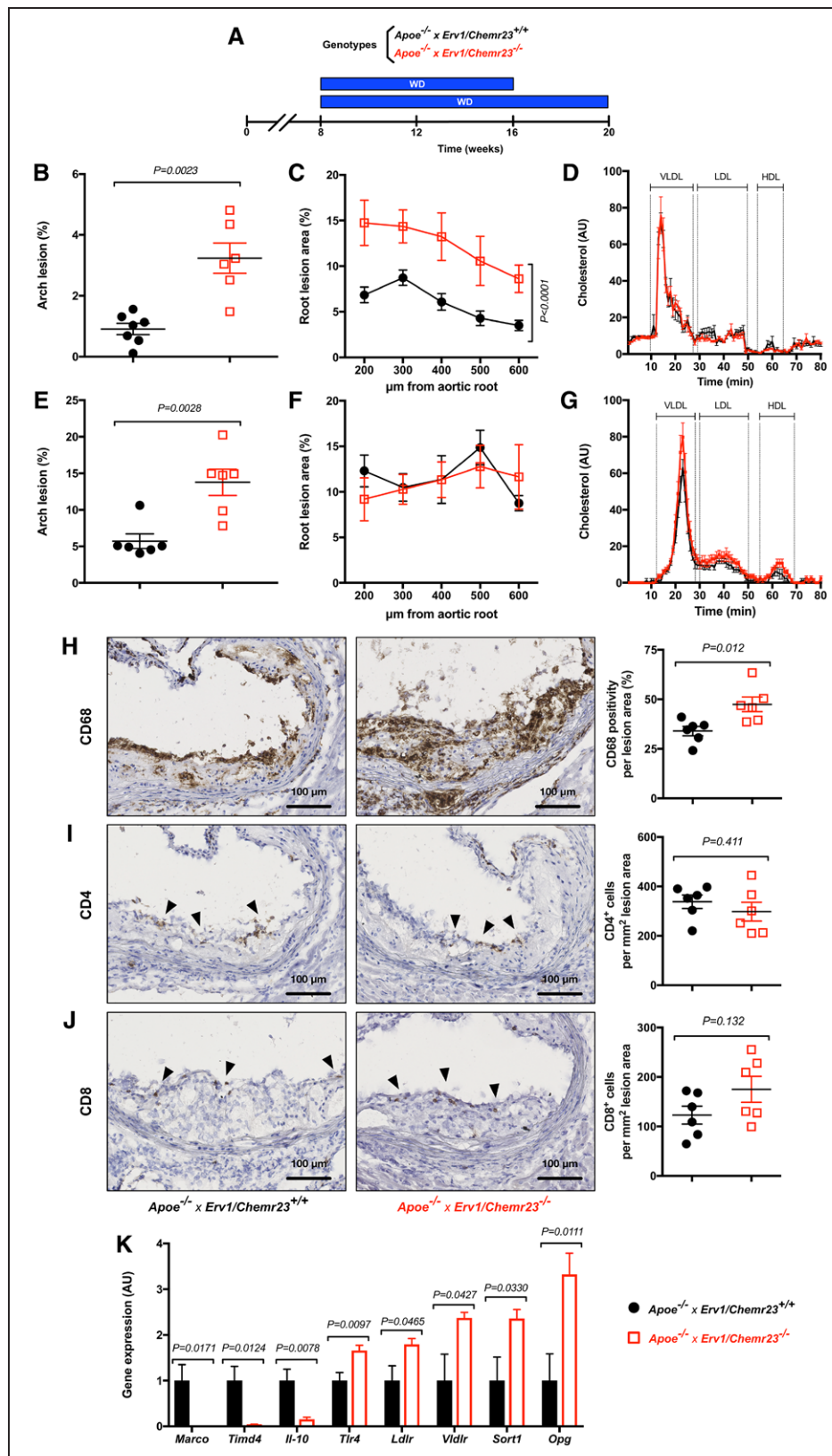


Figure 2. Targeted deletion of *Erv1/ChemR23* in *Apoe*^{-/-} mice enhances atherosclerosis and promotes changes in plaque composition and gene expression.

A, *Apoe*^{-/-}*xErv1/ChemR23*^{+/+} and *Apoe*^{-/-}*xErv1/ChemR23*^{-/-} mice were fed a Western diet 0.15% cholesterol for (B–D) 8 weeks or (E–K) 12 weeks. **B** and **E**, Atherosclerotic lesion size determined as percent of Sudan IV staining of the aortic arch (data presented as mean±SEM; Student *t* test; n=7 versus 6 in **B**, n=6 in **E**) and (C and F) as percent of Oil Red O staining at different levels of the aortic root (data presented as mean±SEM; 2-way ANOVA; n=6). **D** and **G**, Fast protein liquid chromatographic analysis of plasma lipoprotein profiles. Cholesterol concentration in each fraction (y axis) is expressed as mean±SEM in arbitrary (Continued)

(250 nmol/L) significantly decreased oxLDL uptake in control mice, whereas RvE1 did not significantly alter oxLDL uptake in peritoneal macrophages derived from *Apoe*^{-x}*Erv1/Chemr23*^{-/-} mice (Figure 3C).

Peritoneal macrophages obtained from *Apoe*^{-x}*Erv1/Chemr23*^{-/-} mice exhibited reduced phagocytic capacity after 1 hour of incubation with pHrodo-labeled zymosan particles compared with those obtained from control mice (Figure 3D), a difference that persisted over time (Figure 3E). RvE1 (50 nmol/L) significantly increased phagocytosis in wild-type macrophages but did not significantly alter phagocytosis in *Apoe*^{-x}*Erv1/Chemr23*^{-/-} peritoneal macrophages (Figure 3F).

***Erv1/Chemr23*^{-/-} Bone Marrow Confers Increased Atherosclerotic Lesions and Necrotic Core in Chimeric *Ldlr*^{-/-} Mice**

Chimeric animals that received *Erv1/Chemr23*^{-/-} bone marrow exhibited larger atherosclerotic lesions in the aortic root than the control group (Figure 4A and 4B). There were no significant differences in blood counts, weight (Table II in the online-only Data Supplement), plasma triglycerides (4.94±2.2 versus 6.39±1.88 mmol/L; *P*=0.11), total cholesterol (30.14±11.18 versus 35.28±6.35 mmol/L; *P*=0.2027), and lipoprotein profile (Figure 4C) between the groups. A significant increase in necrotic core size was found in *Erv1/Chemr23*^{-/-} chimeras compared with the control group (Figure 4D).

ERV1/ChemR23–Expressing Macrophages Localize in the Proximity of the Necrotic Core in Human Atherosclerotic Plaques

In human atherosclerotic plaques, ERV1/ChemR23 immunoreactivity was observed mainly in the proximity of the necrotic core and less prominently in the fibrous cap (Figure 5A). Smooth muscle actin–positive smooth muscle cells expressed ERV1/ChemR23 in the fibrous cap (Figure 5B) and media regions (Figure 5C); however, the strongest ERV1/ChemR23 expression was associated with the pan-macrophage marker CD68 and specifically located in the proximity of the necrotic core (Figure 5D). Staining with antibodies against ERV1/ChemR23 and CD163, heme oxygenase 1, and arginase 1 revealed that none of these markers were expressed by ERV1/ChemR23⁺ cells (Figure 5E–5H).

ERV1/ChemR23 Expression in Human Atherosclerotic Plaques Is Associated With Key Genes for Lipoprotein Uptake and Phagocytosis

ERV1/ChemR23 expression exhibited significant, albeit moderate, inverse associations with *LDLR*, *VLDLR*, and *SORT1* and was significantly positively associated with *TMD4* and *MARCO* (Figure 5I).

Statin Users Exhibit Higher ERV1/ChemR23 Expression in Their Atherosclerotic Plaques

Stratification of the cohort according to the use of statins revealed that *ERV1/ChemR23* expression was significantly higher in statin users compared with non-users, whereas age, sex, body mass index, weight, concurrent diabetes mellitus, smoking, plasma levels of triglycerides, high-density lipoprotein, high-sensitivity C-reactive protein, fibrinogen, creatinine, and estimated glomeruli filtration rate were not significantly different between the 2 groups (Table 3). As expected, plasma total cholesterol and LDL cholesterol were significantly reduced in statin users.

DISCUSSION

The present study provides a link among EPA supplementation, the generation of the precursors of proresolving lipid mediators, and their signaling pathways in the context of cardiovascular disease. Specifically, we identify 18-HEPE as a plasma biosynthetic pathway marker of EPA supplementation. We further characterize the receptor for the 18-HEPE–derived lipid mediator RvE1, ERV1/ChemR23, as a key player in atherosclerosis. Targeted deletion of *Erv1/Chemr23* in 2 independent hyperlipidemic murine models was associated with proatherogenic signaling in macrophages, increased oxLDL uptake, reduced phagocytosis, and increased atherosclerotic plaque size and necrotic core formation. Moreover, we localized ERV1/ChemR23 expression in human atherosclerotic lesions and demonstrated its augmented expression in statin users. Taken together, these results disclose the RvE1 precursor 18-HEPE as a critical plasma marker formed during EPA supplementation and reveal that RvE1 signaling through ERV1/ChemR23 transduces protective effects in atherosclerosis.

Figure 2 Continued. units (AU) and plotted against retention time (x axis). The fractions corresponding to very-low-density lipoprotein (VLDL), low-density lipoprotein (LDL), and high-density lipoprotein (HDL) are indicated (2-way ANOVA; *n*=4). **H**, Representative photomicrographs of aortic roots stained with antibodies against CD68 for macrophages, **(I)** CD4, and **(J)** CD8 for different T-cell populations (data presented as mean±SEM; Student *t* test; *n*=6). **K**, Aortic mRNA expression of LDL receptor (*Ldlr*), VLDL receptor (*Vldlr*), sortilin 1 (*Sort1*), macrophage receptor with collagenous structure (*Marco*), T-cell immunoglobulin and mucin domain containing 4 (*Timd4*), osteoprotegerin (*Opg*), Toll-like receptor 4 (*Tlr4*), and interleukin 10 (*Il-10*) (data presented as mean±SEM; Student *t* test; *n*=6).

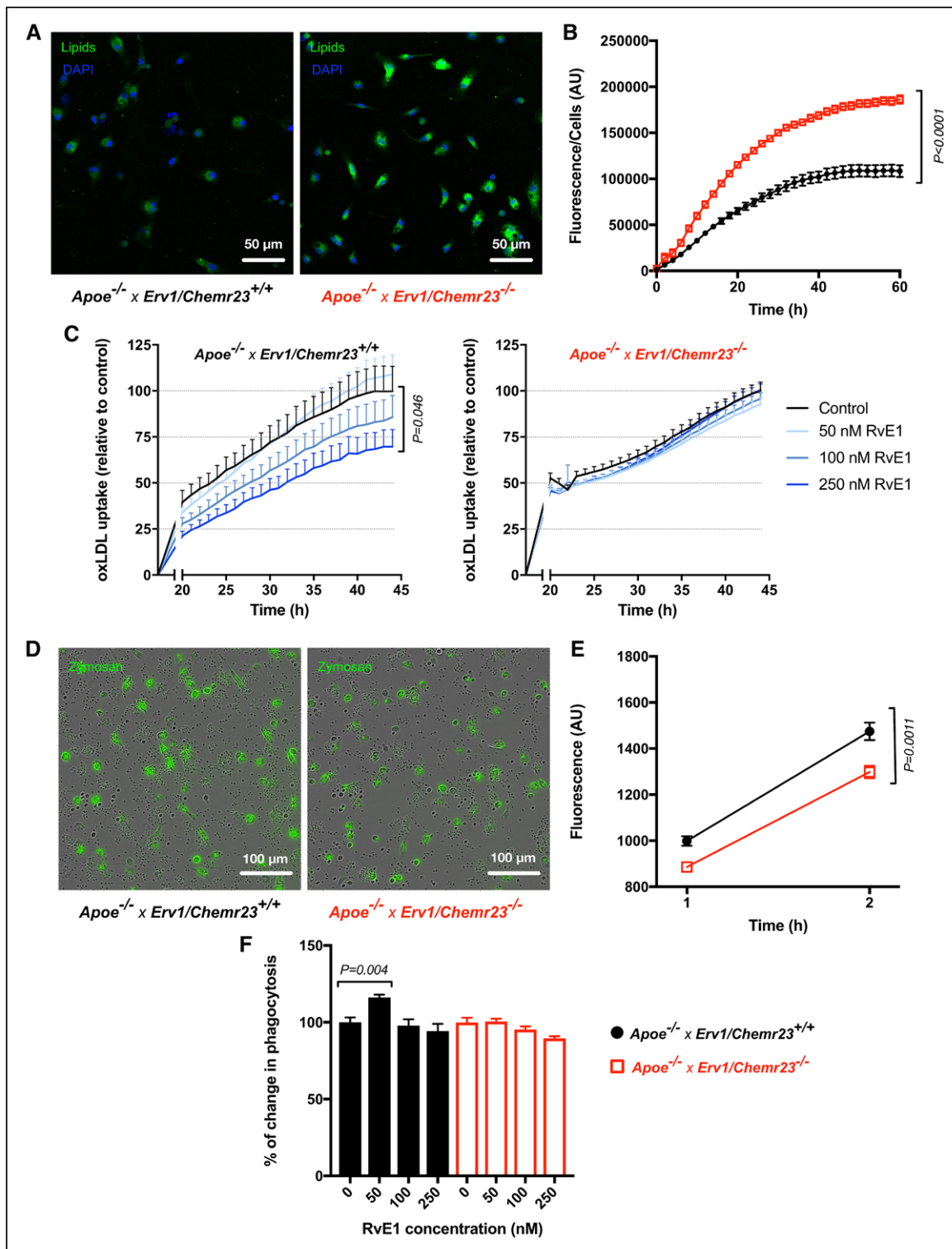


Figure 3. *Apoe*^{-/-}*xErv1/Chemr23*^{-/-} macrophages exhibit increased oxidized low-density lipoprotein (oxLDL) uptake and decreased phagocytosis.

Resolvin E1 (RvE1) effects on oxLDL uptake and phagocytosis are dependent on *Erv1/Chemr23*. **A**, Representative photomicrographs of intracellular lipid content in peritoneal macrophages after 24 hours of incubation with oxLDL using lipophilic fluorophore BODIPY (light gray) and DAPI (dark gray) as nuclei counterstaining. **B**, FITC-labeled oxLDL uptake in peritoneal macrophages. Images were collected every 2 hours for a total of 60 hours (data presented as mean±SEM; 2-way ANOVA; n=3). **C**, Peritoneal macrophages were stimulated with RvE1 (50–250 nmol/L, 15 minutes) followed by coincubation with FITC-labeled oxLDL (10 µg/mL). Images were collected every 1 hour for a total of 45 hours (data presented as mean±SEM; 2-way ANOVA; n=3). **D**, Representative phase-contrast and fluorescence overlay photomicrographs of peritoneal macrophages engulfing pHrodo-labeled zymosan particles (green) after 60 minutes of incubation. **E**, Total fluorescence emitted by macrophages engulfing zymosan particles over time (data shown as mean±SEM; 2-way ANOVA; n=5). **F**, Peritoneal macrophages were stimulated with RvE1 (50–250 nmol/L, 15 minutes) followed by coincubation with pHrodo-labeled zymosan particles for 2 hours (data shown as mean±SEM; 2-way ANOVA; n=3). AU indicates arbitrary units.

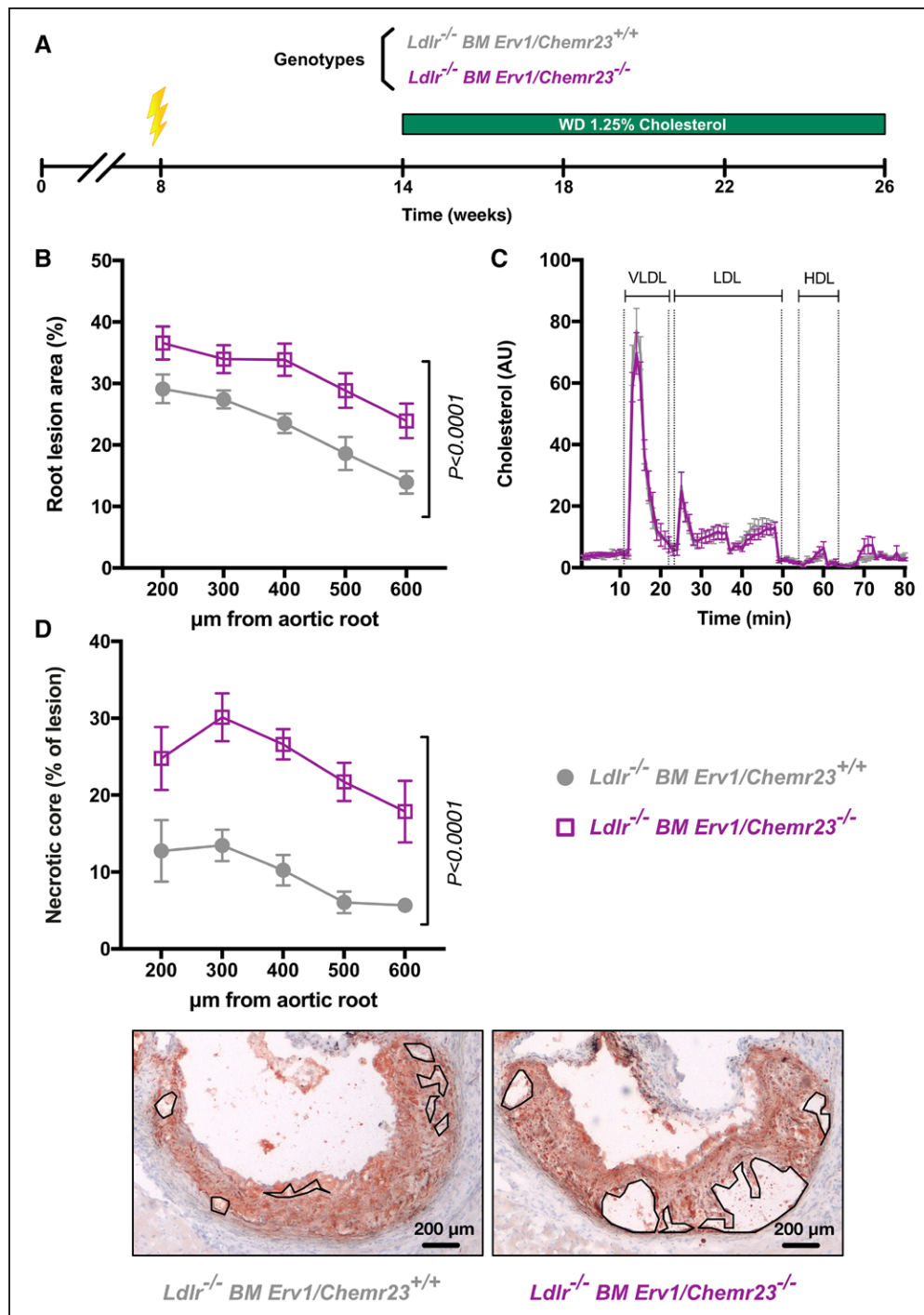


Figure 4. *Erv1/Chemr23*-deficient chimeras display enhanced lesion development and increased necrotic core size.

A, Bone marrow (BM) transplantation experimental design: *Ldlr*^{-/-} mice were lethally irradiated and subsequently transplanted with BM from either *Erv1/Chemr23*^{+/+} or *Erv1/Chemr23*^{-/-} mice. After 6 weeks of recovery, the animals were fed a Western diet 1.25% cholesterol for an additional 12-week period. **B**, Atherosclerotic lesion size determined as percent of Oil Red O staining at different levels of the aortic root (data presented as mean±SEM; 2-way ANOVA; n=7). **C**, Fast protein liquid chromatographic analysis of plasma lipoprotein profiles. Cholesterol concentration in each fraction (y axis) is expressed as mean±SEM in arbitrary units (AU) and plotted against retention time (x axis). The fractions corresponding to very-low-density lipoprotein (VLDL), low-density lipoprotein (LDL), and high-density lipoprotein (HDL) are indicated (2-way ANOVA; n=5). **D**, Necrotic core size determined as percent of lesion in Oil Red O stainings of the aortic root. Representative images showing the necrotic core (areas marked with black lines) from the 2 groups of chimeras.

Our study demonstrates that EPA supplementation caused an attenuation of Western diet-induced atherosclerosis. Despite no significant differences in total cholesterol levels, we observed a reduction in

VLDL cholesterol and in hepatic *Hmgcr* expression in the EPA-supplemented animals. Furthermore, EPA was incorporated into cardiovascular structures, where it may serve as a substrate for lipid mediator formation.

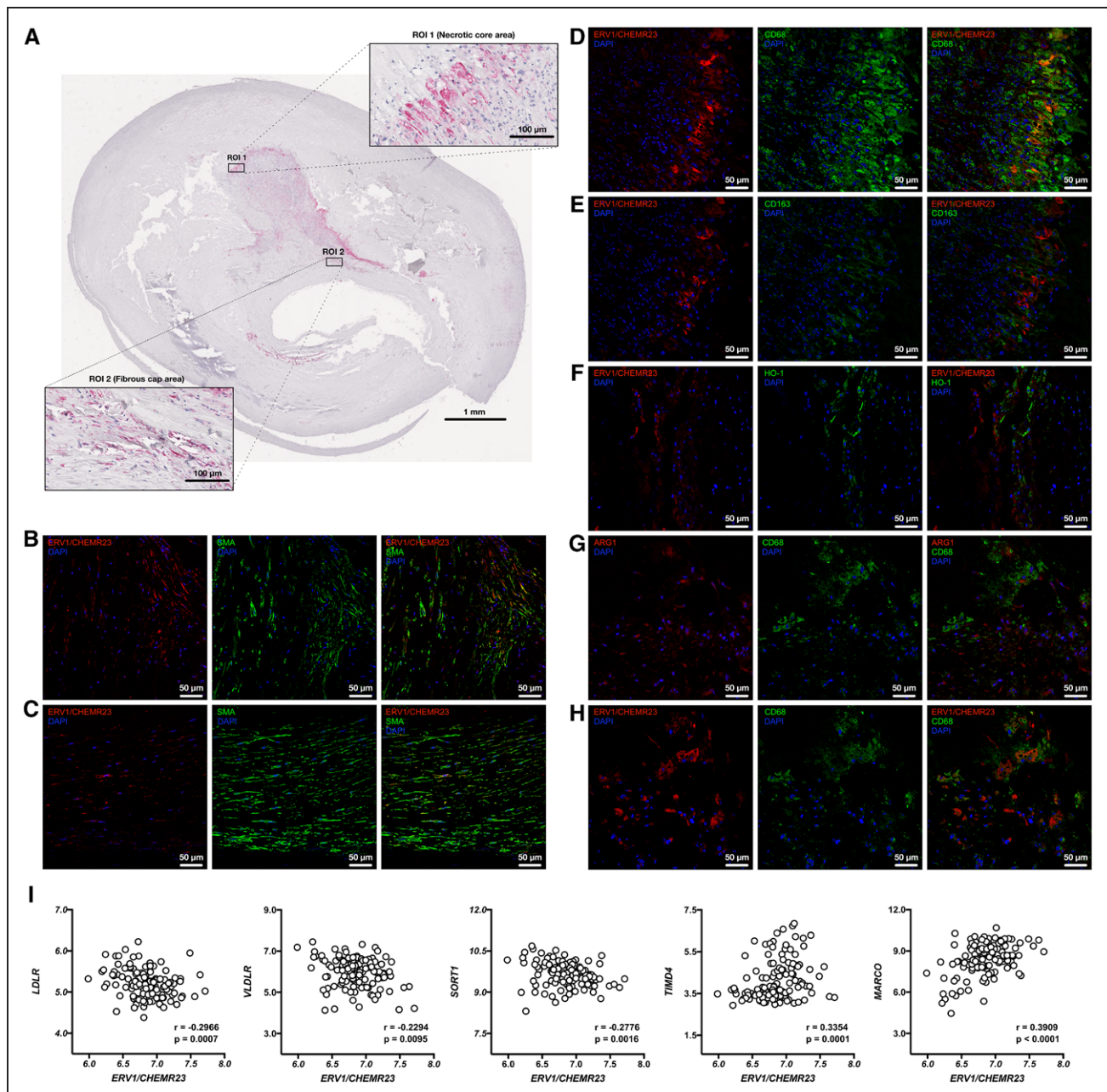


Figure 5. ERV1/ChemR23 expression patterns in human atherosclerotic plaques.

A, Representative photomicrographs of ERV1/ChemR23 immunohistochemical detection in human carotid atherosclerotic lesions. Higher magnification images of 2 regions of interest (ROIs) display the proximity of the necrotic core (ROI 1) and the fibrous cap (ROI 2). **B**, Representative immunofluorescence stainings of smooth muscle cells expressing ERV1/ChemR23 in the fibrous cap and **(C)** media layer. **D** through **H**, Representative immunofluorescence stainings of different macrophage markers and ERV1/ChemR23 in human carotid atherosclerotic plaques. **D** and **H**, ERV1/ChemR23 colocalized with CD68 but not with **(E)** CD163, **(F)** heme oxygenase 1 (HO-1), or **(H)** arginase 1 (ARG1). Consecutive sections were used in **G** and **H**. **I**, ERV1/ChemR23 mRNA expression association (Spearman correlation coefficient; $n=125$) with low-density lipoprotein receptor (*LDLR*), very-low-density lipoprotein receptor (*VLDLR*), sortilin 1 (*SORT1*), macrophage receptor with collagenous structure (*MARCO*), and T-cell immunoglobulin and mucin domain containing 4 (*TIMD4*). SMA indicates smooth muscle actin.

Indeed, n3-derived lipid metabolites were robustly increased in the plasma of EPA-supplemented mice, and 18-HEPE was identified as a critical metabolite formed as a result of this dietary supplementation. Similarly, Endo et al¹⁵ identified 18-HEPE as a key n-3 metabolite in the context of pressure maladaptive cardiac remodeling using a murine strain capable of producing n-3 PUFA endogenously.

The chiral mediator 18-HEPE is the precursor for the short-lived, locally produced, proresolving, anti-inflammatory RvE1. Here, we identify 18S-HEPE as the predominant enantiomer, a relevant observation because that configuration allows the formation of 18S-RvE1, which, compared with the *R* configuration, displays increased affinity and potency for the receptor ERV1/ChemR23.¹¹ It should nonetheless be pointed out that

Table 3. Stratification of Patients Based On Statin Use

| Variable | Statin Use | | P Value |
|--|-------------------|-------------------|---------|
| | No | Yes | |
| Age, y | 72 (67.8–79.5) | 72 (65–78) | 0.5014 |
| Sex, n (%) | | | 0.0991 |
| Male | 20 (16) | 77 (61.6) | |
| Female | 2 (1.6) | 26 (20.8) | |
| Body mass index, kg/m ² | 27 (24.3–28.9) | 25.45 (23.7–28.3) | 0.2007 |
| Weight, kg | 81 (75–88.5) | 77.85 (70–86) | 0.2557 |
| Smoking, n (%) | | | 0.3039 |
| No plus former | 17 (15.0) | 69 (61.1) | |
| Yes | 3 (2.7) | 24 (21.2) | |
| Diabetes mellitus, n (%) | | | 0.1566 |
| No or do not know | 19 (15.2) | 74 (59.2) | |
| Yes | 3 (2.4) | 29 (23.2) | |
| Cholesterol, mmol/L | 5.5 (3.9–6.1) | 4.2 (3.7–4.9) | 0.0266* |
| Low-density lipoprotein cholesterol, mmol/L | 3.6 (2.1–4.3) | 2.2 (1.9–2.8) | 0.0145* |
| High-density lipoprotein cholesterol, mmol/L | 1.05 (0.9–1.3) | 1.2 (0.9–1.4) | 0.4022 |
| Triglycerides, mmol/L | 1.55 (1.1–2.5) | 1.5 (1–2.1) | 0.6787 |
| Fibrinogen, g/L | 3.3 (2.8–4) | 3.6 (3.1–4.5) | 0.3394 |
| High-sensitivity C-reactive protein, mg/L | 4.05 (1.5–9.3) | 2.65 (1.3–6.2) | 0.2882 |
| Creatinine, μ mol/L | 85 (69.8–98.3) | 88 (76–105) | 0.4968 |
| Estimated glomerular filtration rate, mL/min | 81.57 (70.3–98.9) | 75.52 (62.9–88) | 0.1918 |
| <i>Erv1/Chemr23</i> , arbitrary units | 6.69 (6.4–6.9) | 6.86 (6.7–7.1) | 0.0208* |

Categorical data are reported as count (percentage); numerical data are given as median (interquartile range).

*Significant ($P < 0.05$).

both configurations are biologically active and enhance macrophage phagocytosis to a similar extent.¹⁶ Although RvE1 did not appear in the general lipid profiling,¹³ a targeted analysis¹⁴ of spleen tissue revealed increased RvE1 concentrations after EPA supplementation, which may reflect the inherent nature of RvE1 as a locally produced mediator.

These findings taken together, the observed reduction in atherosclerosis after EPA supplementation could hence reflect the decrease in VLDL or a response to EPA-derived lipid mediators. Indeed, previous studies have shown that RvE1 reduces experimental atherosclerosis.^{10,17} However, the role of its receptor *Erv1/Chemr23* has not previously been explored in this context. After having established *Erv1/Chemr23* expression in the aortas of *Apoe*^{-/-} mice and to avoid the possible confounding effect of EPA in lipoprotein metabolism, we generated *Apoe*^{-/-}*xErv1/Chemr23*^{-/-} double-knockout

mice to specifically unveil the *Erv1/Chemr23* signaling pathway in atherosclerosis.

Erv1/Chemr23-deficient mice displayed an accelerated atherosclerosis without alterations in plasma lipids, which was observed at different time points and replicated in a separate series. In an advanced stage of the disease, the difference in lesion size between the 2 genotypes persisted in the aortic arch but not in the root, probably reflecting a plateau phase in lesion growth at this site. Lesion composition analyses revealed an increase in macrophage infiltration, accompanied by significant changes in aortic gene expression in a proinflammatory manner through the upregulation of *Opg*, and *Tlr4* and downregulation of *Il-10*^{18–20} in *Erv1/Chemr23*-deficient mice. Additional significantly increased expression of genes involved in macrophage lipoprotein uptake such as *Ldlr*, *Vldlr*, and *Sort1*^{21–24} and reduction of genes involved in phagocytosis such as *Timd4* and *Marco*^{25,26} were found in *Erv1/Chemr23*-deficient mice.

On the basis of those findings, we investigated the processes of oxLDL uptake and phagocytosis in peritoneal macrophages and demonstrated that *Erv1/Chemr23*-deficient macrophages exhibit enhanced oxLDL uptake and decreased phagocytosis, supporting the notion that macrophage *Erv1/Chemr23* signaling may transduce protective effects in atherosclerosis. Those observations were further supported by the decreased oxLDL uptake and enhanced macrophage phagocytosis induced by its ligand RvE1 in the present study. These effects of RvE1 were not observed in *ERV1/ChemR23*-deficient macrophages, which underlines the beneficial effects of RvE1 signaling through *ERV1/ChemR23* in atherosclerosis. This also lays the foundation for a new function in resolution biology, namely that, in addition to anti-inflammation and enhanced phagocytosis, pro-resolving RvE1 signaling by means of *ERV1/ChemR23* may directly decrease oxLDL uptake, which would be expected to limit inflammatory activation and potentially reduce antigen presentation and activation of adaptive immune circuits.¹

To further consolidate this notion, we replicated the increased atherosclerosis lesion size by transfer of *Erv1/Chemr23*^{-/-} bone marrow into *Ldlr*^{-/-} mice in an advanced stage of the disease. In this model, a remarkable increase in the size of the necrotic core, consistent with our in vitro findings, was also observed. Taken together, these results support the notion that *ERV1/ChemR23* plays a critical role in macrophage-specific oxLDL uptake and phagocytosis and that it offers protection against lesion development and necrotic core formation.

It has previously been established that macrophages in human aortic and coronary atherosclerotic lesions express *ERV1/ChemR23*,²⁷ and this finding was replicated in carotid endarterectomies in the present study. We

show that ERV1/ChemR23 was expressed by a subset of CD68⁺ macrophages residing in the proximity of the necrotic core. This subpopulation of cells was negative for markers of the M2 and Mox macrophage phenotype,²⁸ suggesting that ERV1/ChemR23 expression may be specific for a phagocytic macrophage population associated with the necrotic core. The transcriptomic profile of human carotid lesions revealed that *ERV1/ChemR23* expression was negatively associated with *LDLR*, *VLDLR*, and *SORT1* and positively associated with *TIMD4* and *MARCO*, hence supporting the results obtained in the mouse models and encouraging an extrapolation of the beneficial effects of ERV1/ChemR23 signaling to human atherosclerosis. The latter suggestion is further strengthened by our observation that *ERV1/ChemR23* mRNA levels were significantly higher in carotid endarterectomies derived from statin users compared with those from patients who did not receive these medications. The observational nature of these human data, however, means that no conclusions of causality can be drawn, and the moderate associations observed should be acknowledged as a limitation. Nevertheless, *ERV1/ChemR23* upregulation by statin treatment has been demonstrated in human macrophages,²⁹ which hence may account for additional enhancement of proresolving pathways in atherosclerosis.

Although the significance of ERV1/ChemR23 signaling has been established in liver and adipose tissue metabolism,^{30,31} the present study is the first to demonstrate the importance of this receptor for atherosclerosis. In contrast, targeting another receptor that transduces lipid mediators and peptide signaling, ALX/FPR2, has generated contradictory results in atherosclerosis,^{11,32–34} thus illustrating the complexity of the signaling induced by its different ligands. It should be mentioned that, in addition to 18-HEPE-derived RvE1, other ligands for ERV1/ChemR23 exist^{35,36} and may be involved in the generation of the observed phenotype in *Erv1/Chemr23*-deficient mice. Indeed, we also established differences in chemerin levels resulting from the type of diet, which may further enhance ERV1/ChemR23 signaling in atherosclerosis.

CONCLUSIONS

This study confirms that EPA supplementation attenuates diet-induced atherosclerosis in *ApoE*^{-/-} mice, associated with local cardiovascular n-3 enrichment and altered lipoprotein metabolism. We extend previous observations by identifying the RvE1 precursor 18-HEPE as a central plasma metabolite formed during EPA supplementation to hyperlipidemic mice. We provide the first evidence for a major role of the RvE1 receptor *Erv1/Chemr23* in antiatherogenic macrophage signaling by means of promoting anti-inflammation, decreasing ox-LDL uptake, and enhancing phagocytosis, with implica-

tions for atherosclerotic lesion size, plaque macrophage content, and necrotic core formation. Finally, we provide the translational implications of these findings by identifying a specific ERV1/ChemR23-expressing macrophage subtype in the proximity of the necrotic core in human atherosclerotic lesions and its association with lipoprotein uptake and phagocytic markers, as well as an increased *ERV1/ChemR23* expression in the plaques of the patients receiving statins. ERV1/ChemR23 signaling pathway may represent a novel potential therapeutic target to reduce atherosclerotic cardiovascular disease.

ARTICLE INFORMATION

Received November 16, 2017; accepted April 20, 2018.

The online-only Data Supplement is available with this article at <https://www.ahajournals.org/doi/suppl/10.1161/circulationaha.117.032801>.

Correspondence

Magnus Bäck, MD, PhD, Translational Cardiology, Department of Medicine, Norrbacka S1:02, Karolinska University Hospital, Karolinska Institute, Stockholm, Sweden. E-mail magnus.back@ki.se

Affiliations

Experimental Cardiovascular Research, Department of Medicine (A.L.-F., M.C., G.A., M.H.P., R.B., M.J.F., X.J., T.A., H.A., A.G., S.T., G.P.-B., D.F.J.K., G.K.H., M.B.), Division of Physiological Chemistry II, Department of Medical Biochemistry and Biophysics (A.C., C.E.W.), and Heart and Vascular Theme, Division of Valvular and Coronary Disease (M.B.), Karolinska Institutet, Stockholm, Sweden. Biochemical Pharmacology, William Harvey Research Institute, Barts and the London School of Medicine, Queen Mary University of London, United Kingdom.

Acknowledgments

The authors acknowledge Solutex GC for providing Omegatex9000EE, Omegatrix GmbH for performing the fatty acid analyses, and the supporting staff at the Center for Molecular Medicine.

Sources of Funding

This work was supported by the Swedish Research Council (grant 2014-2312), the Swedish Heart and Lung Foundation (grants 20150600 and 20150683), Marianne and Marcus Wallenberg Foundation (grant MMW 2015.0104), King Gustaf V and Queen Victoria Freemason Foundation, and the Stockholm County Council (grant 20170365). Dr Laguna-Fernandez was supported by a fellowship from the Center of Excellence for Research on Inflammation and Cardiovascular Disease (CERIC Linnaeus Program, grant 349-2007-8703) and funds from Nanna Svartz Fond, Fredrik och Ingrid Thuring's Stiftelse, Stiftelsen för Gamla Tjänarinnor, and Foundation for Geriatric Diseases at Karolinska Institutet. Dr Jesmond Dalli was supported by a Sir Henry Dale Fellowship jointly funded by the Wellcome Trust and the Royal Society (grant number: 107613/Z/15/Z), funding from the European Research Council (ERC) under the European Union's Horizon 2020 research and innovation programme (grant number: 677542), and the Barts Charity (grant number: MGU0343).

Disclosures

None.

REFERENCES

- Libby P, Ridker PM, Hansson GK. Progress and challenges in translating the biology of atherosclerosis. *Nature*. 2011;473:317–325. doi: 10.1038/nature10146.
- Ridker PM, Everett BM, Thuren T, MacFadyen JG, Chang WH, Ballantyne C, Fonseca F, Nicolau J, Koenig W, Anker SD, Kastelein JJP, Cornel JH, Pais P, Pella D, Genest J, Cifkova R, Lorenzatti A, Forster T, Kobalava Z,

- Vida-Simiti L, Flather M, Shimokawa H, Ogawa H, Dellborg M, Rossi PRF, Troquay RPT, Libby P, Glynn RJ; CANTOS Trial Group. Antiinflammatory therapy with canakinumab for atherosclerotic disease. *N Engl J Med*. 2017;377:1119–1131. doi: 10.1056/NEJMoa1707914.
3. Serhan CN. Pro-resolving lipid mediators are leads for resolution physiology. *Nature*. 2014;510:92–101. doi: 10.1038/nature13479.
 4. Merched AJ, Ko K, Gotlinger KH, Serhan CN, Chan L. Atherosclerosis: evidence for impairment of resolution of vascular inflammation governed by specific lipid mediators. *FASEB J*. 2008;22:3595–3606. doi: 10.1096/fj.08-112201.
 5. Fredman G, Spite M. Specialized pro-resolving mediators in cardiovascular diseases. *Mol Aspects Med*. 2017;58:65–71. doi: 10.1016/j.mam.2017.02.003.
 6. Serhan CN, Clish CB, Brannon J, Colgan SP, Chiang N, Gronert K. Novel functional sets of lipid-derived mediators with antiinflammatory actions generated from omega-3 fatty acids via cyclooxygenase 2-nonsteroidal antiinflammatory drugs and transcellular processing. *J Exp Med*. 2000;192:1197–1204.
 7. Arita M, Bianchini F, Aliberti J, Sher A, Chiang N, Hong S, Yang R, Petasis NA, Serhan CN. Stereochemical assignment, antiinflammatory properties, and receptor for the omega-3 lipid mediator resolvin E1. *J Exp Med*. 2005;201:713–722. doi: 10.1084/jem.20042031.
 8. Herrera BS, Hasturk H, Kantarci A, Freire MO, Nguyen O, Kansal S, Van Dyke TE. Impact of resolvin E1 on murine neutrophil phagocytosis in type 2 diabetes. *Infect Immun*. 2015;83:792–801. doi: 10.1128/IAI.02444-14.
 9. Gao L, Faibish D, Fredman G, Herrera BS, Chiang N, Serhan CN, Van Dyke TE, Gyurko R. Resolvin E1 and chemokine-like receptor 1 mediate bone preservation. *J Immunol*. 2013;190:689–694. doi: 10.4049/jimmunol.1103688.
 10. Hasturk H, Abdallah R, Kantarci A, Nguyen D, Giordano N, Hamilton J, Van Dyke TE. Resolvin E1 (RvE1) attenuates atherosclerotic plaque formation in diet and inflammation-induced atherogenesis. *Arterioscler Thromb Vasc Biol*. 2015;35:1123–1133. doi: 10.1161/ATVBAHA.115.305324.
 11. Petri MH, Laguna-Fernandez A, Arnardottir H, Wheelock CE, Perretti M, Hansson GK, Bäck M. Aspirin-triggered lipoxin A4 inhibits atherosclerosis progression in apolipoprotein E-/- mice. *Br J Pharmacol*. 2017;174:4043–4054. doi: 10.1111/bph.13707.
 12. Siscovick DS, Barringer TA, Fretts AM, Wu JH, Lichtenstein AH, Costello RB, Kris-Etherton PM, Jacobson TA, Engler MB, Alger HM, Appel LJ, Mozaffarian D; American Heart Association Nutrition Committee of the Council on Lifestyle and Cardiometabolic Health; Council on Epidemiology and Prevention; Council on Cardiovascular Disease in the Young; Council on Cardiovascular and Stroke Nursing; and Council on Clinical Cardiology. Omega-3 polyunsaturated fatty acid (fish oil) supplementation and the prevention of clinical cardiovascular disease: a science advisory from the American Heart Association. *Circulation*. 2017;135:e867–e884. doi: 10.1161/CIR.0000000000000482.
 13. Balgoma D, Yang M, Sjödin M, Snowden S, Karimi R, Levänen B, Merikalio H, Kaarteenaho R, Palmberg L, Larsson K, Erle DJ, Dahlén SE, Dahlén B, Sköld CM, Wheelock AM, Wheelock CE. Linoleic acid-derived lipid mediators increase in a female-dominated subphenotype of COPD. *Eur Respir J*. 2016;47:1645–1656. doi: 10.1183/13993003.01080-2015.
 14. Dalli J, Colas RA, Quintana C, Barragan-Bradford D, Hurwitz S, Levy BD, Choi AM, Serhan CN, Baron RM. Human sepsis eicosanoid and pro-resolving lipid mediator temporal profiles: correlations with survival and clinical outcomes. *Crit Care Med*. 2017;45:58–68. doi: 10.1097/CCM.0000000000002014.
 15. Endo J, Sano M, Isobe Y, Fukuda K, Kang JX, Arai H, Arita M. 18-HEPE, an n-3 fatty acid metabolite released by macrophages, prevents pressure overload-induced maladaptive cardiac remodeling. *J Exp Med*. 2014;211:1673–1687. doi: 10.1084/jem.20132011.
 16. Oh SF, Pillai PS, Recchiuti A, Yang R, Serhan CN. Pro-resolving actions and stereoselective biosynthesis of 18S E-series resolvins in human leukocytes and murine inflammation. *J Clin Invest*. 2011;121:569–581. doi: 10.1172/JCI42545.
 17. Salic K, Morrison MC, Verschuren L, Wielinga PY, Wu L, Kleemann R, Gjørstrup P, Kooistra T. Resolvin E1 attenuates atherosclerosis in absence of cholesterol-lowering effects and on top of atorvastatin. *Atherosclerosis*. 2016;250:158–165. doi: 10.1016/j.atherosclerosis.2016.05.001.
 18. Perez de Ciriza C, Lawrie A, Varo N. Osteoprotegerin in cardiometabolic disorders. *Int J Endocrinol*. 2015;2015:564934.
 19. Roshan MH, Tambo A, Pace NP. The role of TLR2, TLR4, and TLR9 in the pathogenesis of atherosclerosis. *Int J Inflamm*. 2016;2016:1532832. doi: 10.1155/2016/1532832.
 20. Caligiuri G, Rudling M, Ollivier V, Jacob MP, Michel JB, Hansson GK, Nicoletti A. Interleukin-10 deficiency increases atherosclerosis, thrombosis, and low-density lipoproteins in apolipoprotein E knockout mice. *Mol Med*. 2003;9:10–17.
 21. Herijgers N, Van Eck M, Groot PH, Hoogerbrugge PM, Van Berkel TJ. Low density lipoprotein receptor of macrophages facilitates atherosclerotic lesion formation in C57Bl/6 mice. *Arterioscler Thromb Vasc Biol*. 2000;20:1961–1967.
 22. Eck MV, Oost J, Goudriaan JR, Hoekstra M, Hildebrand RB, Bos IS, van Dijk KW, Van Berkel TJ. Role of the macrophage very-low-density lipoprotein receptor in atherosclerotic lesion development. *Atherosclerosis*. 2005;183:230–237. doi: 10.1016/j.atherosclerosis.2005.03.045.
 23. Patel KM, Strong A, Tohyama J, Jin X, Morales CR, Billheimer J, Millar J, Kruth H, Rader DJ. Macrophage sortilin promotes LDL uptake, foam cell formation, and atherosclerosis. *Circ Res*. 2015;116:789–796. doi: 10.1161/CIRCRESAHA.116.305811.
 24. Pirault J, Polyzos KA, Petri MH, Ketelhuth DFJ, Bäck M, Hansson GK. The inflammatory cytokine interferon-gamma inhibits sortilin-1 expression in hepatocytes via the JAK/STAT pathway. *Eur J Immunol*. 2017;47:1918–1924. doi: 10.1002/eji.201646768.
 25. Foks AC, Engelbertsen D, Kuperwaser F, Alberts-Grill N, Gonen A, Witztum JL, Lederer J, Jarolim P, DeKruyff RH, Freeman GJ, Lichtman AH. Blockade of Tim-1 and Tim-4 enhances atherosclerosis in low-density lipoprotein receptor-deficient mice. *Arterioscler Thromb Vasc Biol*. 2016;36:456–465. doi: 10.1161/ATVBAHA.115.306860.
 26. Jing J, Yang IV, Hui L, Patel JA, Evans CM, Prikeris R, Kobzik L, O'Connor BP, Schwartz DA. Role of macrophage receptor with collagenous structure in innate immune tolerance. *J Immunol*. 2013;190:6360–6367. doi: 10.4049/jimmunol.1202942.
 27. Kostopoulos CG, Spiroglou SG, Varakis JN, Apostolakis E, Papadaki HH. Chemerin and CMKLR1 expression in human arteries and periaortic fat: a possible role for local chemerin in atherosclerosis? *BMC Cardiovasc Disord*. 2014;14:56. doi: 10.1186/1471-2261-14-56.
 28. Tabas I, Bornfeldt KE. Macrophage phenotype and function in different stages of atherosclerosis. *Circ Res*. 2016;118:653–667. doi: 10.1161/CIRCRESAHA.115.306256.
 29. Tuomisto TT, Lumivuori H, Kansanen E, Häkkinen SK, Turunen MP, van Thienen JV, Horrevoets AJ, Levonen AL, Ylä-Herttua S. Simvastatin has an anti-inflammatory effect on macrophages via upregulation of an atheroprotective transcription factor, Kruppel-like factor 2. *Cardiovasc Res*. 2008;78:175–184. doi: 10.1093/cvr/cvn007.
 30. López-Vicario C, Rius B, Alcaraz-Quiles J, González-Pérez A, Martínez-Puchol AI, Casulleras M, Duran-Güell M, Ibarzabal A, Corcelles R, Laguna-Fernández A, Back M, Titos E, Clària J. Association of a variant in the gene encoding for ERV1/ChemR23 with reduced inflammation in visceral adipose tissue from morbidly obese individuals. *Sci Rep*. 2017;7:15724. doi: 10.1038/s41598-017-15951-z.
 31. Ernst MC, Issa M, Goralski KB, Sinal CJ. Chemerin exacerbates glucose intolerance in mouse models of obesity and diabetes. *Endocrinology*. 2010;151:1998–2007. doi: 10.1210/en.2009-1098.
 32. Petri MH, Laguna-Fernández A, Gonzalez-Diez M, Paulsson-Berne G, Hansson GK, Bäck M. The role of the FPR2/ALX receptor in atherosclerosis development and plaque stability. *Cardiovasc Res*. 2015;105:65–74. doi: 10.1093/cvr/cvu224.
 33. Fredman G, Kamaly N, Spolitu S, Milton J, Ghorpade D, Chiasson R, Kuria-kose G, Perretti M, Farokhzad O, Tabas I. Targeted nanoparticles containing the proresolving peptide Ac2-26 protect against advanced atherosclerosis in hypercholesterolemic mice. *Sci Transl Med*. 2015;7:275ra20. doi: 10.1126/scitranslmed.aaa1065.
 34. Drechsler M, de Jong R, Rossaint J, Viola JR, Leoni G, Wang JM, Grommes J, Hinkel R, Kupatt C, Weber C, Döring Y, Zarbock A, Soehnlein O. Annexin A1 counteracts chemokine-induced arterial myeloid cell recruitment. *Circ Res*. 2015;116:827–835. doi: 10.1161/CIRCRESAHA.116.305825.
 35. Ferland DJ, Watts SW. Chemerin: A comprehensive review elucidating the need for cardiovascular research. *Pharmacol Res*. 2015;99:351–361. doi: 10.1016/j.phrs.2015.07.018.
 36. Peng L, Yu Y, Liu J, Li S, He H, Cheng N, Ye RD. The chemerin receptor CMKLR1 is a functional receptor for amyloid-β peptide. *J Alzheimers Dis*. 2015;43:227–242. doi: 10.3233/JAD-141227.